Solid State Communications 151 (2011) 826–829

Contents lists available at ScienceDirect

Solid State Communications

journal homepage: www.elsevier.com/locate/ssc

Kapitza conductance of Bi/sapphire interface studied by depth- and time-resolved X-ray diffraction

Y.M. Sheu [a,*], M. Trigo [b,c], Y.J. Chien [d], C. Uher [d], D.A. Arms [e], E.R. Peterson [e], D.A. Walko [e], E.C. Landahl [f], J. Chen [b,c], S. Ghimire [b,c], D.A. Reis [b,c]

[a] FOCUS Center and Department of Physics, University of Michigan, Ann Arbor, MI 48109-1040, USA
[b] PULSE Institute, SLAC National Accelerator Laboratory Menlo Park, CA 94025, USA
[c] Departments of Photon Science and Applied Physics, Stanford University, Stanford, CA 94305, USA
[d] Department of Physics, University of Michigan, Ann Arbor, MI 48109-1040, USA
[e] Argonne National Laboratory, Argonne, IL 60439, USA
[f] Department of Physics, DePaul University, Chicago, IL 60614, USA

ARTICLE INFO

Article history:
Received 12 March 2011
Accepted 21 March 2011
by R. Merlin
Available online 2 April 2011

Keywords:
A. Bismuth
D. Kapitza conductance
E. Ultrafast
E. X-rays

ABSTRACT

We present Kapitza conductance measurements of the bismuth/sapphire interface using depth- and time-resolved X-ray diffraction, for Bi film thicknesses ranging from 65 to 284 nm. Our measurements provide complementary information about heat transport in the films; we directly observe the thinnest film to be uniformly heated within 1 ns, whereas the thickest film sustains a large near-surface temperature gradient for several ns. The deduced Kapitza conductance is 1950 W/cm^2/K. This value is close to the theoretical prediction using the radiation limit.

The thermal boundary (Kapitza) conductance across an interface between dissimilar materials gives rise to a temperature discontinuity during heat flow and is a limiting factor in the thermal transport in nanoscale devices [1,2]. Fundamentally, the Kapitza conductance is limited by the transmission of phonons across the interface and is thus sensitive to the detailed characteristics of an interface. Understanding phonon transmission across an interface, especially in nanoscale or complex heterostructures, can advance device fabrication for efficient energy conversion. Phonon transmission across an interface is also a fundamental physical problem related to the scattering processes. For purely elastic scattering (no phonon conversion across an interface), the maximum Kapitza conductance occurs when phonon transmission is unity for all phonons with frequency lower than the smaller Debye cutoff frequency between two sides of the interface. This upper limit often provides a simple yet useful estimation for the Kapitza conductance when the operating temperature falls between the Debye temperatures of the two materials, the so -called radiation limit [3]. Various optical pump–probe measurements have reported Kapitza conductances across highly dissimilar materials which exceeds this value, often by an order of magnitude [3,4]. In this letter, we report measurements of the Kapitza conductance close to the radiation limit for a bismuth (Debye temperature $\Theta_D = 120$ K) and sapphire ($\Theta_D = 1024$ K) interface using an alternative method, time-resolved X-ray diffraction (TRXD). Depth- and time-resolved X-ray diffraction was previously used by Johnson et al. [5] for studying coherent optical phonon dynamics in bismuth. We show that it also provides complementary information about heat transport across a heterostructure following impulsive heating from ultrafast laser absorption. Using a combination of grazing incidence and symmetric diffraction on several film thicknesses, we directly observe that thermal transport is dominated initially by the thermal conductance of the bismuth film and later dominated by the Kapitza conductance as heat flows to the sapphire substrate.

Bi films of 65, 141, and 284 nm thickness were grown on 1 × 1 cm^2 sapphire substrates (c-axis 001 cut, ∼0.5 mm thick) by molecular beam epitaxy (MBE). The films were single crystals with the c (trigonal) axis perpendicular to the surface as determined by X-ray diffraction. In this letter, we use hexagonal representation with Miller indices (hkl) and lattice constants (a, a, c) for the following discussion.

Experiments were conducted near room temperature on the 7ID insertion device beamline at the Advanced Photon Source

* Corresponding author. Tel.: +1 734 330 8215.
E-mail address: ymsheu@lanl.gov (Y.M. Sheu).

0038-1098/$ – see front matter © 2011 Elsevier Ltd. All rights reserved.
doi:10.1016/j.ssc.2011.03.022

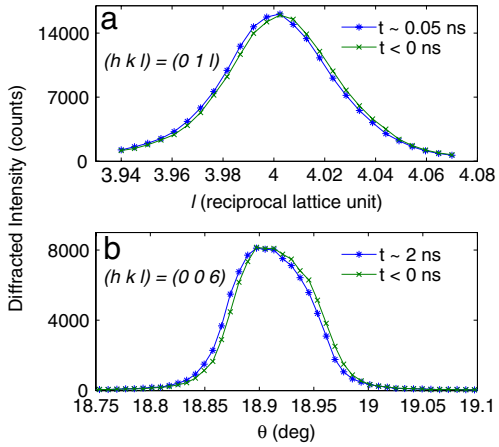

Fig. 1. (Color online) (a) Miller index l versus diffracted intensity from asymmetric Bi(014) diffraction. (b) Angle versus diffracted intensity from symmetric Bi(006) diffraction. Both show the Bragg peak with laser after and laser before X-rays.

synchrotron. A detailed description of the beamline, in the context of ultrafast experiments, can be found elsewhere [6–11]. 10 keV and 7 keV X-ray pulses were used for symmetric and asymmetric diffraction measurements, respectively. Amplified Ti:sapphire laser pulses were centered at 800 nm with ~50 fs pulse duration at a 5 kHz repetition rate. The detailed timing scheme and normalization for X-rays due to bunch-to-bunch fluctuation can be found in Ref. [9]. The spot size for the laser pump was $\sim 0.2 \times 0.2\ \mathrm{cm}^2$ and for the X-ray probe is $\sim 100 \times 300\ \mu\mathrm{m}^2$. Approximately 0.2–0.4 $\mathrm{mJ/cm}^2$ laser fluence was absorbed in the films typically.

We used symmetric diffraction at the (006) Bragg peak to probe lattice changes averaged over the entire film and used asymmetric Bi(014) diffraction to study depth-resolved lattice changes at various X-ray incident angles, both studying lattice changes along the c axis. We label the diffraction planes using hexagonal indices. Grazing incident angles of $\alpha = 0.4°$, 0.5°, 3°, and 6° were used for asymmetric diffraction, corresponding to X-ray extinction depths of approximately 3.5, 12, 160, and 320 nm respectively. The Bi(014) and Bi(006) diffraction peaks are displayed in Fig. 1, both shown with the comparison before heating ($t < 0$) and after heating ($t > 0$) by the laser pulses. Any change to lattice spacing after laser excitation at these time delays was due to the change in lattice temperature, which is estimated to average ~26, 12, 6 K in uniformly heated 65, 141, 284 nm thick films, respectively, from ~0.2 $\mathrm{mJ/cm}^2$ absorbed fluence. Note that when the sample is heated by ultrafast laser, the near-surface temperature could be much higher than these average values in early times, due to strong absorption at 800 nm for Bi.

In hexagonal representation, the Bragg peak position measured by uniaxial strain $\Delta d/d$ along the c-axis and the change in the Miller index l is related as $\Delta d/d = -(d^2/c^2) \times l\Delta l$. For a Gaussian-like X-ray peak profile, the change in peak intensity at l near half maximum is approximately linear to the peak shift Δl. For the asymmetric diffraction measurements, we use this intensity shift to study the lattice change which is proportional to the temperature change via the linear expansion coefficient. For symmetric diffraction, the change in the Bragg angle and in lattice constant are connected through $\Delta\theta = -(\Delta d/d)\tan\theta_B$. The change in the Bragg angle is, therefore, a direct measurement for temperature change.

Fig. 2 shows the normalized intensity near the half-maximum of the (014) peak as a function of pump–probe delay for the 65 nm (a) and 284 nm (b) films. In each case, the signal increases suddenly as the film is heated followed by a relatively slow decay. For the 65 nm film, the decay is independent of the grazing angle after ~1 ns, indicating that the film is heated more or less uniformly on

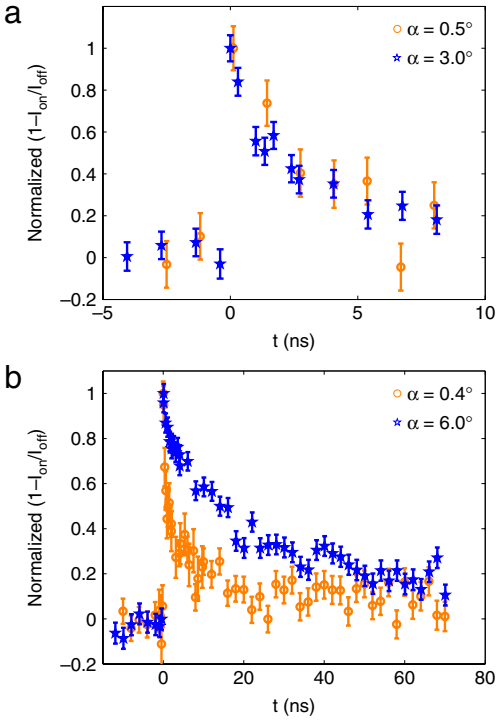

Fig. 2. (Color online) Diffracted intensity change as a function of time at various grazing incident angles from $(hkl) = (0\ 1\ 4.012)$ for film thickness (a) 65 nm and (b) 284 nm.

this time scale. This is consistent with an estimate for the diffusion time ~0.65 ns, i.e. $t \sim L^2/4D$, estimated from the bulk thermal diffusivity D for bismuth and film thickness L. Therefore, the cooling for the 65 nm film measured by depth- and time-resolved X-ray diffraction is dominated by the Kapitza conductance. In contrast, the thermal decay of the 284 nm film, shown in Fig. 2b, depends strongly on the grazing incidence angle. This is to be expected for the thicker film, in which the diffusion time of ~12 ns is comparable to the decay measured with $\alpha = 0.4°$. Thus, for the 284 nm film, the cooling from the near surface region at early times is attributed to thermal diffusion that homogenizes the temperature profile across the film. At later times and as we probe deeper into the film, the decay becomes more and more sensitive to the Kapitza conductance.

Since probing deeper is more sensitive to the Kapitza conductance, we use (006) symmetric diffraction to measure the lattice change averaged over the entire film. Fig. 3 displays cooling for three films of varying thickness. Due to the much larger pump size than the probe size, during the time scale of our measurements the transport is mainly along the sample normal. The plateau at early times is due to a temperature redistribution which maintains the same average temperature throughout the depth of the film, resulting in a good agreement with diffusion time constants estimated using bulk lattice thermal conductivity. To extract the Kapitza conductance, we numerically solve the one-dimensional diffusion equation:

$$\frac{dT(t,z)}{dt} = \frac{\kappa}{C}\frac{d^2T(t)}{dz^2} \tag{1}$$

for both film and substrate with boundary conditions

$$C\frac{dT(t)}{dt} = -\sigma\left.\frac{dT}{dz}\right|_{z=L}, \tag{2}$$

$$\left.\frac{dT}{dz}\right|_{z=0} = 0, \tag{3}$$

and initial temperature profile in the film

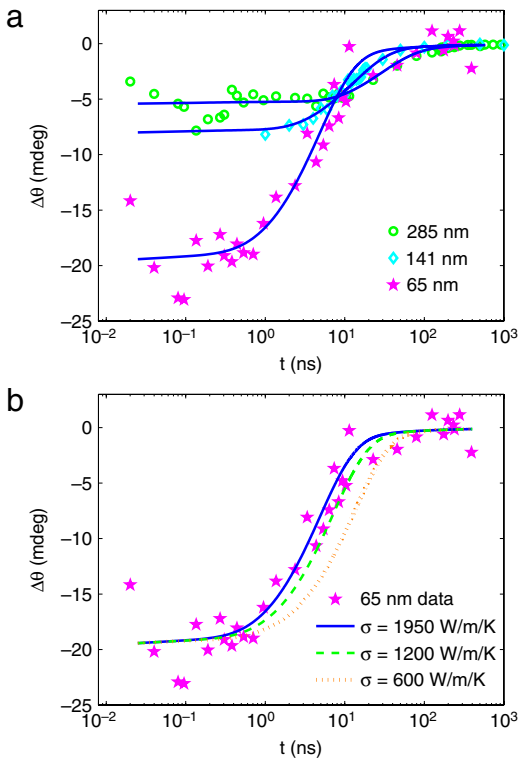

Fig. 3. (Color online) (a) Time-resolved Bragg angle shift from 006 diffraction for three different film thicknesses. The solid lines are best fit ($\sigma = 1950$ W/cm^2/K) using the solution to the thermal diffusion equation as described in the text. (b) Comparison of sensitivity between different Kapitza conductances for 65 nm film.

$$\Delta T_f(z, t = 0) = T_0\, e^{-z/\xi}, \tag{4}$$

where C, κ, and T_0 are heat capacity, lattice thermal conductivity, and initial maximum temperature rise, respectively, with the film surface at $z = 0$ and interface at $z = L$. Using bulk lattice thermal conductivity for Bi with free parameters σ and T_0, the best fit for Kapitza conductance across the Bi/sapphire interface is 1950 W/cm^2/K averaged from the three films.

The result is not sensitive to the initial temperature profile which could be altered by the fast electronic transport. The maximum change in angle shift at a fixed fluence is nearly inversely proportional to the film thickness, since the temperature averaged over the entire film is inversely linear to film thickness. We have done temperature calibration by attaching a thermometer on the back of a sample holder and measuring the angle shift of Bi(006) diffraction when the sample is uniformly heated by an external heat source. The measured temperature from the thermometer is averaged over the angle scan, and the static angle shift as a function of temperature is shown in Fig. 4. The straight line is the theoretical value calculated from

$$\Delta\theta = -\alpha\, \Delta T \left(\frac{1+\nu}{1-\nu}\right) \tan\theta_B \tag{5}$$

with Bi linear expansion coefficient $\alpha = 13.4 \times 10^{-6}$ K^{-1}, Bragg peak from current experiment $\theta_B = 18.92°$, and Poisson ratio $\nu = 0.33$. The maximum shift corresponds to average temperature ~10, 16, and 38 K for 285, 184, and 65 nm film, respectively, interpolated or extrapolated from Fig. 4 and agrees with numerical estimation when 0.3–0.4 mJ/cm^2 is absorbed. In addition, we note that our measurements of the Kapitza conductance have no explicit dependence on the absorbed fluence up to ~0.8 mJ/cm^2, above which the sample shows damage and the diffraction peak has a broadened tail with reduced peak intensity.

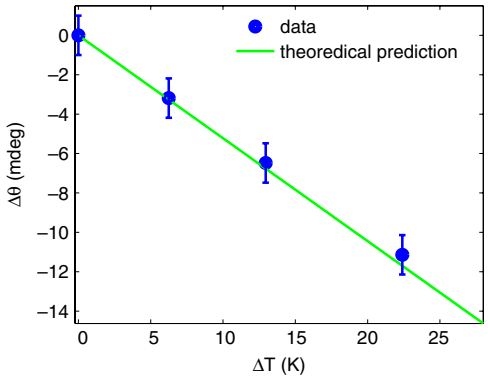

Fig. 4. (Color online) Angle shift as a function of temperature change as entire sample is uniformly heated by an external heat source. The temperature change $\Delta T = 0$ is relative to room temperature. The straight line is the theoretical prediction at our experimental angle of Bi(006) diffraction.

The derived value of σ from experiment is close to but greater than the theoretical prediction using the radiation limit, which is the maximum conductance assuming elastic scattering. Using $\Theta_D = 120$ K for Bi and 1.08×10^6 longitudinal (v_l) and 0.64×10^6 cm/s transverse (v_t) sound velocity for sapphire [3], the estimation for Kapitza conductance using radiation limit is [4]

$$\sigma = \frac{\pi k_B v_{\text{cut}}^3}{c_D^2}, \tag{6}$$

where v_{cut} is cutoff frequency for Bi and c_D is Debye velocity for sapphire defined as $3/c_D^2 = 1/v_l^2 + 2/v_t^2$ in Ref. [4]. The calculated result is $\sigma = 1300$ W/cm^2/K. The Debye temperature of Bi corresponds to a cutoff frequency ~2.5 THz which does not account for the phonon dispersion. In the case of Bi, a simplistic application of the Debye theory fails since it does not account for the phonon dispersion in the relatively complex crystal structure of Bi. It is known from Raman scattering that the A_{1g} phonon is populated at room temperature with frequency about 2.93 THz. If we use A_{1g} frequency instead of Debye cutoff frequency for Eq. (6), we can simply show that the Kapitza conductance $\sigma = 2060$ W/cm^2/K, which is more consistent with our measurement. However, both results, using the Debye cutoff and the A_{1g} phonon frequency, are within the asymmetric error bars of our measurement.

In conclusion, we have used depth- and time-resolved X-ray diffraction to study the thermal transport across the Bi/sapphire interface, directly measuring lattice change as a function of time. Similar decay curves for the 65 nm film, both averaged near the surface and averaged over the entire thickness, indicate a nearly uniform temperature distribution across the film after 1 ns. Therefore, the measured cooling curve for the 65 nm film is dominated by Kapitza conductance after 1 ns. In contrast, the measured cooling for the 284 nm film averaged near the surface within the first few nanoseconds is dominated by thermal conductivity, whereas the cooling averaged near the surface at late times and that averaged over the entire film are dominated by the Kapitza conductance. The Kapitza conductance extracted from symmetric diffraction is 1950 W/cm^2/K averaged from various films, which within the error bar is close to a simple theoretical prediction using the radiation limit and is independent of excitation density below damage threshold.

Use of the Advanced Photon Source, an Office of Science User Facility operated for the US Department of Energy (DOE) Office of Science by Argonne National Laboratory, was supported by the US DOE under Contract No. DE-AC02-06CH11357. This work was supported in part by the US DOE, Grants No. DE-FG02-00ER1503, and from the NSF FOCUS physics frontier center. YJC and CU acknowledge the support from NSF-DMR-0604549. DAR was supported in part by the Air Force Office of Scientific Research

under Contract FA9550-08-1-0340 through the Multidisciplinary University Research Initiative Program.

References

[1] D.G. Cahill, et al., J. Appl. Phys. 93 (2003) 793.
[2] E.T. Swartz, et al., Rev. Modern Phys. 61 (1989) 605.
[3] R.J. Stoner, et al., Phys. Rev. B 48 (1993) 16373.
[4] H.-K. Lyeo, et al., Phys. Rev. B 73 (2006) 144301.
[5] S.L. Johnson, et al., Phys. Rev. Lett. 100 (2008) 155501.
[6] D.A. Reis, et al., Phys. Rev. Lett. 86 (2001) 3072.
[7] M.F. DeCamp, et al., J. Synchrotron Radiat. 12 (2005) 172.
[8] S.H. Lee, et al., Phys. Rev. Lett. 95 (2005) 246104.
[9] Y.M. Sheu, et al., Phys. Rev. B 78 (2008) 045317.
[10] M. Trigo, et al., Phys. Rev. Lett. 101 (2008) 025505.
[11] E. Dufresne, et al., AIP Conf. Proc. 1234 (2010) 181.